4400

Physical Model of an Air-Conditioned Space for Control Analysis

Masato Kasahara
Associate Member ASHRAE

Yoshiaki Kuzuu

Tadahiko Matsuba
Associate Member ASHRAE

Yukihiro Hashimoto
Member ASHRAE

Kazuyuki Kamimura
Member ASHRAE

Shigeru Kurosu, Ph.D.
Member ASHRAE

ABSTRACT

This paper describes a procedure for deriving a dynamic model of an air-conditioned room (space) by applying physical laws to it. The room under control is divided into five zones. The dynamics of each zone can be described by a lumped-capacity model, and a total of 15 linear differential equations can be obtained. The model parameters derived from this procedure can be numerically related to the overall heat transfer coefficients for the room, and the various significant time constants associated with the room envelope. The numerical model can be successfully reduced to a well-known first-order lag plus deadtime system. Proportional-plus-integral (PI) controllers must be designed by estimating deadtimes, time constants, and gain constants of the system. Indoor temperature and relative humidity may be maintained at setpoint values by an air-handling unit using a PI control action. The PI parameters must be carefully tuned to produce a less oscillatory response. The tuning technique, using the partial model matching method, is investigated from a practical viewpoint. A mathematical model of the heating, ventilating, and air-conditioning (HVAC) system, which consists of an air-conditioned room, an air-handling unit, and PI controllers is developed. Simulation results showing the closed-loop responses of indoor temperature and indoor relative humidity are given. The controllable regions on a psychrometric chart are established to demonstrate the practical applicability of our simplified dynamic model. This modeling procedure can be especially useful for control strategies that require knowledge of the dynamic characteristics of HVAC systems.

INTRODUCTION

Successful design of control systems depends mainly on a mathematical model derived by control engineers to achieve accurate control performance. The complexity of an HVAC system, with distributed parameters, interactions, and multivariables, makes it extremely difficult to obtain an exact mathematical model to improve control quality.

The authors have proposed a modeling procedure for the HVAC system taking the multivariable AR (autoregressive) model into account by using experimental data (Kimbara et al. 1995). The effectiveness of the model was clarified by carrying out actual control. However, some of the more important questions were left open:

- When the operating points of the indoor/outdoor temperature and indoor/outdoor humidity change, different models were obtained.
- The order of model generally tended to be very high when evaluation of the model's validity failed.
- For the model derived from statistical approach, it could not be explained how the model parameters correspond to actual performance data of the building.

In recent years, a growing interest in the mathematical modeling of HVAC systems has been seen. Many researchers have reported room models developed through a theoretical approach (Borresen 1981; Zaheer-Uddin and Zheng 1994; Zhang and Nelson 1992; Crawford and Woods 1985; Shavit 1995; Nelson 1965). Their interests were centered on strategies to represent the complete performance of a building and to evaluate energy costs and thermal loads, etc. The mathe-

Masato Kasahara is an assistant in the Department of Electronic Control Engineering and **Shigeru Kurosu** is a professor in the Department of Mechanical Engineering at Oyama National College of Technology, Oyama, Japan. **Yoshiaki Kuzuu** is a graduate student in the Department of Mechanical Systems Engineering at Tokyo University of Agriculture and Technology. **Tadahiko Matsuba** is a control engineer and **Kazuyuki Kamimura** is a manager in the Research and Development Division at Yamatake Building Systems Co., Ltd., Tokyo, Japan. **Yukihiko Hashimoto** is a senior engineer in the Engineering Project Department at Tonets Corporation, Tokyo.

matical models that include the interactions between a building, its occupants, control systems, and the external environment are complex and constantly changing. Although these models may be adequate for building design purposes, none of them seems to give insightful results for a room model, which has an important role in good control performance. This paper discusses a simplified dynamic room model that takes into account the energy and mass balances between room air and the surrounding walls and explains why a control system might not provide the desired performance.

The process of modeling a room involves the following steps:

- Divide the air-conditioned room into several simplified well-mixed zones (the indoor temperature and humidity are the same throughout the zone).
- Model the resulting zones by applying physical laws to the ideal models.
- Analyze the resulting model to determine its properties.
- Reduce the order of the model if necessary so that it is tractable to tune PI controllers.
- Simulate the physical model on a computer to show the closed-loop responses.
- Establish the attainable (or controllable) regions on a psychrometric chart.

This work leads to a better understanding of such thermal properties as thermal capacities and heat transfer coefficients on control performance. This simplified model provides a theoretical foundation for more elaborate models to quantitatively evaluate the overall HVAC control systems.

SYSTEM DESCRIPTION

Figure 1 shows a schematic diagram of the typical VAV (variable air volume) system considered in this study. Since the VAV system is mainly a cooling system, our physical model will be limited to the cooling mode. The major components of the system are (1) an air-conditioned room, (2) an air-handling unit, and (3) a fan and ductwork. The airflow rate to the room is controlled by dampers and/or by fan speed control.

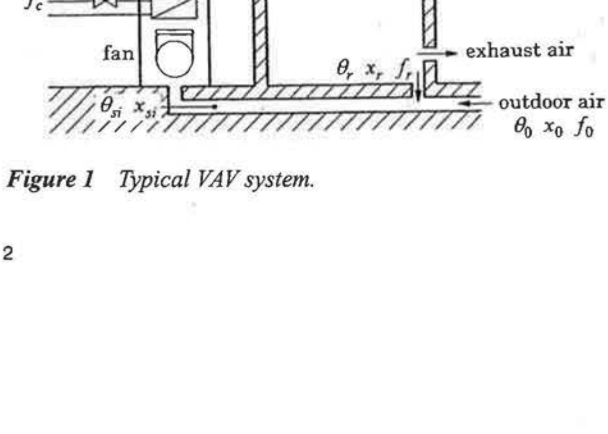

Figure 1 *Typical VAV system.*

The room measures 2 m (L) by 2.5 m (W) by 2.5 m (H) and is connected to the air-handling unit (control element), which consists of a cooling water valve and a humidifier to control indoor temperature and relative humidity. Air enters the cooling coil at a given temperature, which decreases as the air passes through the coil. The thermometer in the downstream side of the coil senses the temperature of the air leaving the coil. Using the output from the sensor, the controller modifies the openings of a control valve. This control valve changes the chilled water flow through the cooling coil. The supply air leaving the coil enters the humidifier, which generates vapor to control indoor humidity. The hygrometer in the room senses relative humidity and then is fed back to the controller. Using this error signal, the controller produces a controlling input as the flow rate of steam. These control units are collectively referred to as an air-handling unit.

The room air is released continuously at the end of the ceiling and drawn into the end of the floor. The airflow rate from the air-handling unit to the room is 4 m^3/min. The airflow rate from the outdoor air inlet is 1 m^3/min and the same rate is usually exhausted into the outdoors. The thermal load in the room consists of one resident only. Thus, there are three control inputs, namely, the supply air temperature, the supply air humidity, and the airflow rate, which can be changed simultaneously in response to variable cooling loads acting on the room. But the current analysis assumes that the supply air temperature is fixed at 10°C. The outputs of interest are the temperature and relative humidity in the room.

The interactions between every component must be considered so that a change in any one input can be used to influence the system outputs, such as indoor temperature and relative humidity. With this as the motivation, we develop zone models that describe the functional relationships between appropriate inputs and outputs.

Zone Model

Since an air-conditioned room is a complex thermal system, a completely theoretical approach to formulating a model is impractical. A set of simultaneous partial differential equations that describe the dynamic balance of energy and mass within the room easily can come out to be intractable. However, dividing this room into five small zones enclosed by envelopes that are exposed to a certain outdoor condition is reasonable. Figure 2 depicts five divisions of the room and five zones—designated 1, 2, 3, 4, and 5—are noted.

The room description follows:

Walls and ceiling: foaming urethane 50 mm thick

Floor: concrete with 50 mm thick insulation

Window: glazing 0.5 m × 0.5 m × 3 mm thick

Occupant: one person in the interior zone (zones 3, 4, and 5)

Equipment: lighting, 240 W bulb, and 1 KW heater (for disturbance inputs)

The following assumptions are made at the start:

1. The air of each zone is fully mixed. Thus, the dynamics of each zone can be expressed in a lumped capacity model and usually yield a rational transfer function.
2. The airflow between two zones is unilateral—the state of the upstream zone is not affected by the state of the downstream zone.
3. Any other uncontrolled inputs, such as extreme weather conditions, internal load upsets, and solar radiation, are considered as disturbance inputs.
4. The density of air is considered to be constant, although the density is a function of temperature and humidity.
5. The pressure losses across zones and in the mixing sections are negligible.

The main reason for these assumptions is to obtain simple models for treating the fundamental issues in control system design. Here, based on these assumptions, typical heat and mass flows within the room are shown in Figure 3.

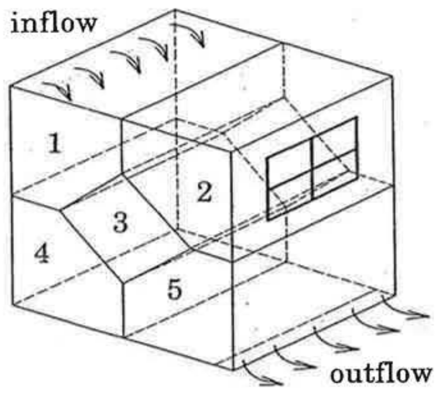

Figure 2 *Zone model.*

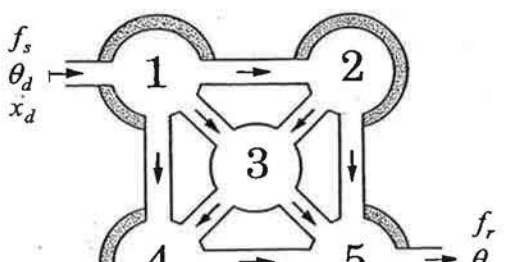

Figure 3 *Heat and mass flows within a room.*

We characterize zone models by three state variables: indoor temperature θ_i, wall temperature θ_{wi}, and indoor absolute humidity x_i of zone i. The governing equations of zone models can be derived by applying the principles of energy and mass balance. By neglecting back currents among zones and assuming perfect mixing for each zone, we lump the thermal capacitance and the volume into five zones.

Heat balance of the air:

$$\left.\begin{aligned} C_1\dot{\theta}_1 &= w\theta_d - w\theta_1 + \alpha_1(\theta_{w1} - \theta_1) \\ C_2\dot{\theta}_2 &= \frac{w}{3}\theta_1 - \frac{w}{3}\theta_2 + \alpha_2(\theta_{w2} - \theta_2) \\ C_3\dot{\theta}_3 &= \frac{w}{3}\theta_1 + \frac{w}{6}\theta_2 - \frac{w}{2}\theta_3 + \alpha_3(\theta_{w3} - \theta_3) + q(t) \\ C_4\dot{\theta}_4 &= \frac{w}{3}\theta_1 + \frac{w}{4}\theta_3 - \frac{7w}{12}\theta_4 + \alpha_4(\theta_{w4} - \theta_4) \\ C_5\dot{\theta}_5 &= \frac{w}{6}\theta_2 + \frac{w}{4}\theta_3 - \frac{7w}{12}\theta_4 - w\theta_5 + \alpha_5(\theta_{w5} - \theta_5) \end{aligned}\right\} \quad (1)$$

Heat balance of the wall:

$$\left.\begin{aligned} C_{w1}\dot{\theta}_{w1} &= \alpha_1(\theta_1 - \theta_{w1}) + \beta_1(\theta_0 - \theta_{w1}) \\ C_{w2}\dot{\theta}_{w2} &= \alpha_2(\theta_2 - \theta_{w2}) + \beta_2(\theta_0 - \theta_{w2}) \\ C_{w3}\dot{\theta}_{w3} &= \alpha_3(\theta_3 - \theta_{w3}) + \beta_3(\theta_0 - \theta_{w3}) \\ C_{w4}\dot{\theta}_{w4} &= \alpha_4(\theta_4 - \theta_{w4}) + \beta_4(\theta_0 - \theta_{w4}) \\ C_{w5}\dot{\theta}_{w5} &= \alpha_5(\theta_5 - \theta_{w5}) + \beta_5(\theta_0 - \theta_{w5}) \end{aligned}\right\} \quad (2)$$

Mass balance of the water vapor:

$$\left.\begin{aligned} V_1\dot{x}_1 &= f_s x_d - f_s x_1 \\ V_2\dot{x}_2 &= \frac{f_s}{3}x_1 - \frac{f_s}{3}x_2 \\ V_3\dot{x}_3 &= \frac{f_s}{3}x_1 - \frac{f_s}{6}x_2 - \frac{f_s}{2}x_3 + \frac{1}{\rho_a}p(t) \\ V_4\dot{x}_4 &= \frac{f_s}{3}x_1 - \frac{f_s}{4}x_3 - \frac{7f_s}{12}x_4 \\ V_5\dot{x}_5 &= \frac{f_s}{6}x_2 - \frac{f_s}{4}x_3 - \frac{7f_s}{12}x_4 + f_s x_5 \end{aligned}\right\} \quad (3)$$

where the dot $(\cdot)$ denotes the time derivative. In Equation 1, the coefficients such as $w/3$, $w/4$, $w/6$, and $7w/12$ can be determined by Kirchhoff's current law: At every instant the amount leaving must equal the amount entering.

Equation 1 states that the rate of change of energy in the zone is equal to the difference between the energy supplied to and removed from the zone, non-temperature-dependent heat gain ($q(t)$), and the heat gain through the envelope, including the warm air infiltration due to the inside-out temperature differential. In Equation 2, the rate of change of energy in the wall ($C_{wi}\dot{\theta}_{wi}$) is equated to the heat gains through the wall between the indoor air and the outdoor air. Similarly, Equation

3 states that the rate of change of moisture in the zone ($V_i\dot{x}_i$) is equal to the difference between the moisture added to and removed from the zone. The room model shows that these zones are unilaterally coupled by input signals w and f_s. The relative humidity (φ) to be controlled in our system is given by a complex function $F(x, \theta)$ of the absolute humidity (x) and the air temperature (θ) (ASHRAE 1989; Wexler and Hyland 1983).

Needless to say any other uncontrolled inputs (e.g., variations of weather conditions, internal load upsets, and solar radiation, etc.) directly or indirectly affect the system dynamics. The radiant energy from those will actually be absorbed in the walls. Thus, extra terms might be added to Equations 1, 2, and 3 if necessary. The addition of the above external thermal influence, however, is seldom of interest in this paper.

By assembling Equations 1 through 3, the overall room model can be easily obtained. All the actual values of the parameters used in the computer simulation are listed in Table 1. The zone model equations may be combined to construct the room model of interest. In order to derive the general form of a first-order ordinary differential equation, let us consider the first three equations of Equation 1. Taking the Laplace transformation of three equations, the following algebraic equations can be obtained:

$$\left.\begin{aligned}(C_1 s + w + \alpha_1)\Theta_1(s) &= w\Theta_d(s) + \alpha_1\Theta_{w1}(s)\\ \left(C_2 s + \frac{w}{3} + \alpha_2\right)\Theta_2(s) &= \frac{w}{3}\Theta_1(s) + \alpha_2\Theta_{w2}(s)\\ \left(C_3 s + \frac{w}{2} + \alpha_3\right)\Theta_3(s) &= \frac{w}{3}\Theta_1(s) + \frac{w}{6}\Theta_2(s) + \alpha_3\Theta_{w3}(s) + Q(s)\end{aligned}\right\} \tag{4}$$

where L denotes the Laplace transform of a function of time, written as $L[\theta_i(t)] = \Theta_i(s)$, $L[\theta_{wi}(t)] = \Theta_{wi}(s)$, $L[q(t)] = Q(s)$, and $L[p(t)] = P(s)$. Similarly, these relations can be expanded to all of Equations 1 through 3. Thus, the causal relationship can be described graphically by the block diagram shown in Figure 4. In this block diagram, the transfer functions are defined by

$$\left.\begin{aligned}G_{w1}(s) = \frac{w}{C_{w1}s + \alpha_1 + \beta_1},\qquad G_1(s) = \frac{w}{C_1 s + w + \alpha_1},\\ H_1(s) = \frac{f}{V_1 s + f}\end{aligned}\right\}, \text{etc.} \tag{5}$$

Also, F in the blocks (Figure 4) represents the nonlinear function $F(x, \theta)$. Note that there are two typical time constants in each zone, namely,

$$T_1 = \frac{C_1}{w + \alpha_1} \text{ and } T_{w1} = \frac{C_{w1}}{\alpha_1 + \beta_1}, \text{etc.} \tag{6}$$

T_1 denotes the air change rate in the room and T_{w1} results in a time constant for the walls. Generally, T_{wi} has a much larger value than T_i as discussed later.

From Figure 4, it should be noted that the signal-flow is strictly unilateral—the condition at the output end of a zone

TABLE 1
Summary of Significant Parameters in the Development of a Room Model

Zone i	1	2	3	4	5
Ci	1.56	21.56	21.56	21.56	
C_{wi}	4.48	4.58	1.53	63.34	63.34
V_i	2.5				
α_i, β_i	0.04	0.06	0.01	0.21	0.21

Air-Handling Unit		Humidifier	
C_a	1.56	C_d	0.052
V_a	1.0	V_d	0.5
α_a	0.78	α_d	0.26

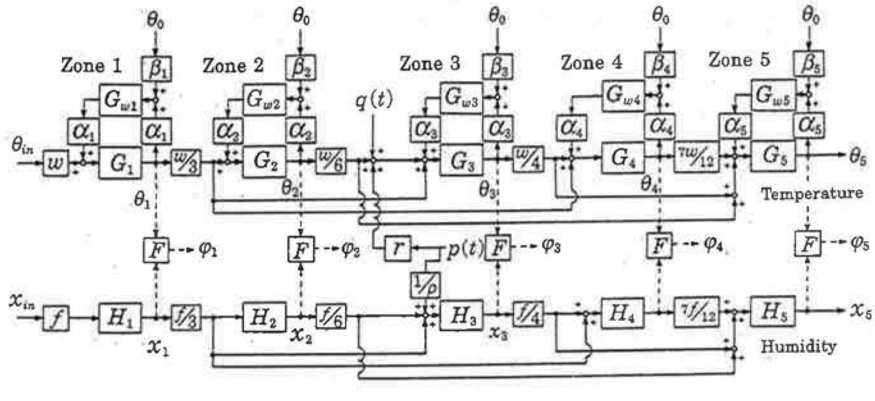

Figure 4 Block diagram of room model.

has no feedback effect on the forward zone. Thus, the room model can be called an open-loop structure. The thermal models (the upper parts shown in Figure 4) interact in some way with the mass flow models (the bottom parts), but the former can be considered independent of the latter because of unilateral coupling.

Air-Handling Unit Model

Cooling Coil Model. For the purpose of modeling the air-handling unit, it is assumed that the unit is full of air at supply temperature and that air density is constant. The cooling water at θ_{ci} is supplied to the cooling coil and returns at a temperature of θ_{co} to the storage tank. By identifying the energy flows to and from the air-handling unit, the energy balance can be expressed by

$$C_a\dot{\theta}_s = -f_c\rho_w c_w(\theta_{co} - \theta_{ci}) + \alpha_a(\theta_o - \theta_s) + f_s\rho_a c_a(\theta_{si} - \theta_s). \quad (7)$$

In Equation 7, the rate of cooling energy stored in the unit is equated to the energy extracted by the cooling pipe and the energy added to the unit via the return air from the room and the surrounding outer surface of the unit. Note that two inputs, f_s (supply airflow rate) and f_c (cooling water flow rate) appear in this equation. The mass balance equation on the water vapor is

$$V_a\dot{x}_s = f_s(x_{si} - x_s). \quad (8)$$

Equation 8 states that the rate of change of moisture in the unit is equal to the difference between water vapor added to and removed from the unit. This implies that, by changing f_s, the mass flow rate to the room can be varied and that water vapor can be stored in the unit.

Model of Airflow in the Duct System. The mass balance equation in the mixing (outdoor air and return air) section is

$$x_{si}f_s = x_o f_o + x_r f_r. \quad (9)$$

The corresponding model equation for the energy balance in the duct can be described by

$$w\theta_{si} = w_o\theta_o + w_r\theta_r. \quad (10)$$

The airflow rate from the outdoor air is considered 25% of the total supply airflow rate. This ratio will be held constant in this study. Note that the pressure losses and the heat losses occurring in the duct are neglected for simplification.

Humidifier Model. Humidification is a requirement in some areas due to the very low humidity that exists in even a cooling mode in winter. The humidifier is the most important interface between the air-handling unit and the room. The humidifier model is separated from the air-handling unit. Since the supply air in the outlet of the unit is usually considered to be saturated vapor (φ_s is 100%) by cooling, the relative humidity of the supply air cannot be controlled by the humidifier in the same air-handling unit. This fact is critically important to successful implementation of an air-handling unit. Simplifying this humidifier exposed to a certain outdoor condition is reasonable.

Here, the energy balance can be expressed by

$$C_d\dot{\theta}_d = w(\theta_s - \theta_d) + \alpha_d(\theta_o - \theta_d). \quad (11)$$

The second term on the right-hand side is the heat gain (or loss) through the humidifier envelope, including the warm infiltration due to the inside-out temperature differential.

The mass balance equation on the water vapor is

$$V_d\dot{x}_d = f_s(x_s - x_d) + \frac{h(t)}{\rho_a}. \quad (12)$$

Note that in Equation 12, the rate of moist air produced in the humidifier $h(t)$ is a function of the indoor relative humidity as one of control inputs. When the supply air becomes saturated vapor (φ_d = 100%), the input $h(t)$ has no effect on the output $x_d(t)$.

Properties of Room Model

By assembling Equations 1 through 3, the overall room model, viz.,

$$\frac{d}{dt}\boldsymbol{x} = \boldsymbol{Ax} + \boldsymbol{Bu} + \boldsymbol{Cd} \quad (13)$$

was obtained, where $\boldsymbol{x}$ is a vector of the state variables, $\boldsymbol{u}$ is a vector of the control inputs and $\boldsymbol{d}$ is a vector of the disturbances. $\boldsymbol{x}$, $\boldsymbol{u}$, and $\boldsymbol{d}$ for this room model are defined by

$$\boldsymbol{x} = [\theta_1, ..., \theta_5, \theta_{w5}, x_1, ..., x_5]^T$$
$$\boldsymbol{u} = [f_s, h]^T \quad (14)$$
$$\boldsymbol{d} = [\theta_0, q, p]^T$$

where T denotes the transpose. The corresponding matrices $\boldsymbol{A}$, $\boldsymbol{B}$, and $\boldsymbol{C}$ can be easily found (Takahashi et al. 1972).

Assuming zero initial conditions, the matrix transfer function is given by

$$\boldsymbol{G}(s) = (s\boldsymbol{I} - \boldsymbol{A})^{-1}\boldsymbol{B} \quad (15)$$

and the characteristic equation is

$$|s\boldsymbol{I} - \boldsymbol{A}| = 0. \quad (16)$$

Hence, using the parameters described in Table 1, a tenth-order characteristic polynomial of the thermal model can be found:

$$\alpha_0 + \alpha_1 s + \alpha_2 s^2 + ... + \alpha_9 s^9 + s^{10} = 0. \quad (17)$$

The location of these roots, which are called characteristic poles, is depicted in Figure 5(a) where R_e means the real part and I_m means the imaginary part. A group of poles lying relatively close to the origin makes the response decay very slow. These long-term responses are due to the thermal dynamics of the wall. On the other hand, all the remaining poles lying along a horizontal axis separate from the origin lead to fast responses that decay rapidly with time. They represent the dynamics of the room. As can be seen from Figure 5, the resulting time constants for the wall (T_{wi}) are larger than those for the room (T_{pi}) by 5 to 100 times. The location of characteristic poles that exclude the wall time constants is shown in Figure 5(b). Neglecting the dynamics of the walls will give a very simple and useful model for short-term responses. For control analysis, the simplified models will often be sufficient. Neglecting the influence of the walls, the transfer function for the thermal model can be reduced into fifth-order systems.

In the tuning control parameters to the dynamics of the plant, which is described by a higher-order transfer function, most plants are approximated by a first-order lag plus deadtime system (Åstoröm and Hägglund 1995). The transfer function comes to

$$G_i(s) = \frac{K_{pi}e^{-L_{pi}s}}{1 + T_{pi}s} \tag{18}$$

where K_{pi}, T_{pi}, and L_{pi} are the gain constant, the time constant,and the deadtime, respectively. A systematic method with which to determine K_{pi}, T_{pi},and L_{pi} by using the parameters is given in the appendix.

The step responses due to a 1°C increase in the supply air temperature are shown in Figure 6. The responses of zones 1 through 5 are marked according to their numbers. The lower curves indicate the responses of the first-order lag plus deadtime system. This approximation is found to be valid for our thermal model.

SIMULATION RESULTS

To show some applications of the developed model, several simulation runs are made for the exact physical model expressed by Equations 1 through 12. The major parameters of the zone models and air-handling unit used in this study are given in Table 1.

Transient Response for an Uncontrolled System

First, the transient responses for an uncontrolled (open-loop) system will be obtained to investigate system performance. The environmental conditions assumed are:

Supply heat energy rate: $w = f_s c_a \rho a = 1.248$ (kcal/min °C)
Supply air temperature: $\theta_s = 10°C$
Supply air absolute humidity: $x_s = 0.008$ (kg/kg (dry air))
Outdoor air temperature: $\theta_o = 32.5°C$
Outdoor air absolute humidity: $x_o = 0.0195$ (kg/kg (dry air))

Also, the initial conditions when $t = 0$ are given by $\theta_i(0) = \theta_{wi}(0) = \theta_o$, $x_i(0) = x_o$ (for $i = 1, 2, ..., 5$).

Equations 1, 2, and 3 are a set of simple first-order differential equations subject to the initial conditions above. The transient responses are illustrated in Figure 7, which shows changes in the indoor temperature, the wall temperature, and the indoor relative humidity. Five zones—designated 1, 2, 3, 4, and 5—are noted in these figures.

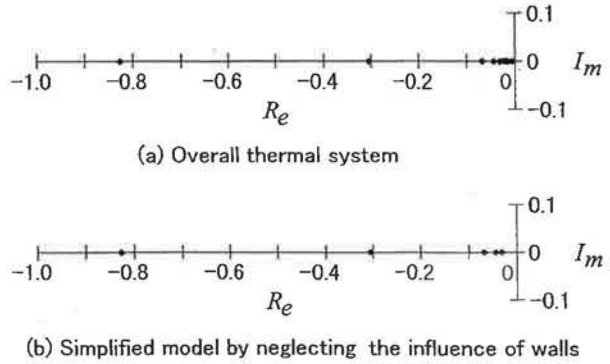

Figure 5 *Location of poles of thermal model.*

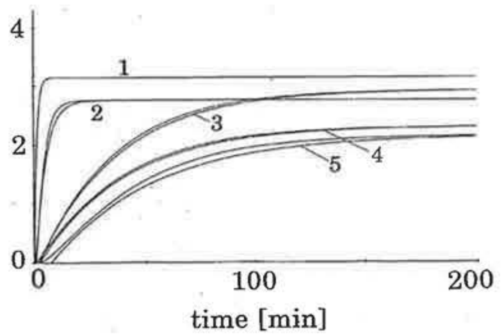

Figure 6 *Comparison of step responses for zones between Equations 19 and 20.*

As can be seen from Figure 7(a), for zones 1 and 2 the temperatures rapidly reach steady-state values because of small heat capacities. But for zones 3, 4, and 5, the responses decrease very slowly depending on large thermal capacities of zones and the cooling loads. It is evident from the results for zones 4 and 5 that the responses are not only influenced by the cooling loads but also by the thermal capacities of floors and walls. Figure 7(b) shows the long-term responses, i.e., the responses over a couple of hours or so due to the large thermal capacities of the walls.

As shown in Figure 7(c), the relative humidities for zones 1 and 2 rise rapidly during the start-up time due to quick cooling of supply air. At this time, the humidities for zones 3, 4, and 5 decrease rapidly due to the thermal loads of a resident and climb slowly following the decrease of the wall temperature.

Transient Response for a Controlled System

In order to maintain the indoor temperature and the indoor relative humidity in desirable ranges, a PI control and I-P control are introduced (see the appendix for a brief review of

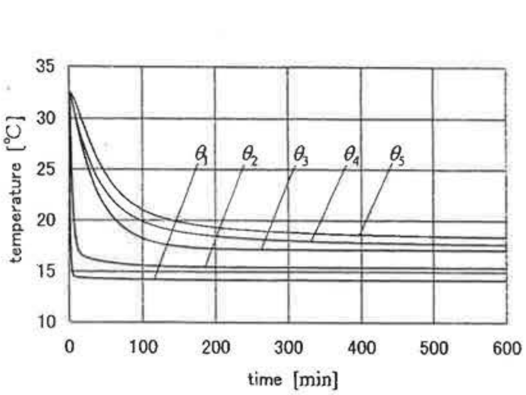

(a) Indoor temperature

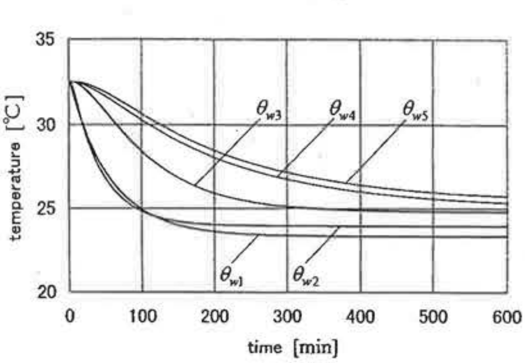

(b) Wall temperature

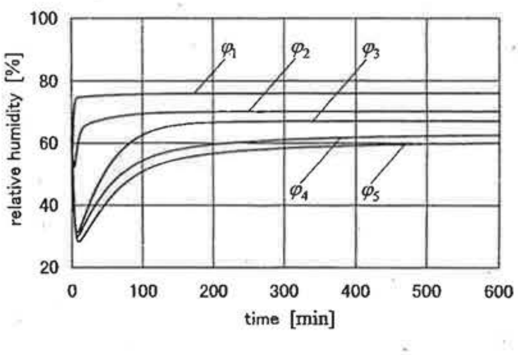

(c) Indoor relative humidity

Figure 7 *Transient responses of an open-loop system.*

the PI and I-P controls). For practical considerations, such as safety and energy savings, I-P control law is generally preferred (Kasahara et al. 1997). The two types of control law are shown schematically in Figure 8. Let us assume two outputs, θ_3 and φ_3, for zone 3 (the central part of the room) as controlled variables to maintain at desired values. For our VAV system, the supply air temperature is assumed to be constant. The control inputs that vary according to the control actions are the supply airflow rate f_s, the supply air absolute

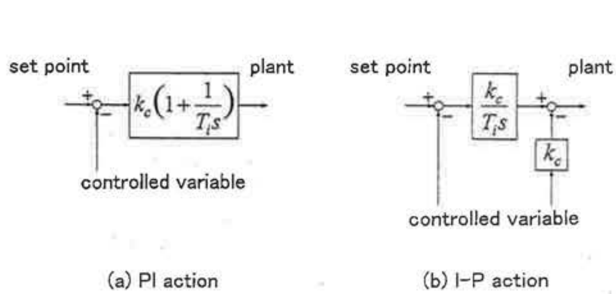

Figure 8 *Block diagrams of control algorithm.*

humidity x_d, and the water flow rate through the cooling coil f_c. For PI controls, the control inputs are given by

$$\left.\begin{aligned} f_s &= k_{c1}\left\{(\theta_3-\theta_r)+\frac{1}{T_{i1}}\int_0^t(\theta_3-\theta_r)dt\right\}, \\ h &= k_{c2}\left\{(\varphi_r-\varphi_3)+\frac{1}{T_{i2}}\int_0^t(\varphi_r-\varphi_3)dt\right\}, \\ f_c &= k_{c3}\left\{(\theta_s-\theta_{sr})+\frac{1}{T_{i3}}\int_0^t(\theta_s-\theta_{sr})dt\right\} \end{aligned}\right\} \tag{19}$$

where θ_r, φ_r, and θ_{sr} are the setpoint values of the indoor temperature, the indoor humidity, and the supply air temperature. For I-P controls, the control inputs can be written similarly,

$$\left.\begin{aligned} f_s &= k_{c1}\left\{\theta_3+\frac{1}{T_{i1}}\int_0^t(\theta_3-\theta_r)dt\right\}, \\ h &= k_{c2}\left\{-\varphi_3+\frac{1}{T_{i2}}\int_0^t(\varphi_r-\varphi_3)dt\right\}, \\ f_c &= k_{c3}\left\{\theta_s+\frac{1}{T_{i3}}\int_0^t(\theta_s-\theta_{sr})dt\right\} \end{aligned}\right\}, \tag{20}$$

where k_{c1}, k_{c2}, and k_{c3} = proportional gains and T_{i1}, T_{i2}, and T_{i3} = integral times.

So-called reset windup can be a problem with PI and IP algorithms above. If the controlled variable cannot be controlled (a damper is wide open, for example) an error may persist, causing the integral summation to increase or to decrease to unreasonable values. To avoid this, the controller locks the integrator at its present value whenever the control output is at an extreme.

The setpoints values of the indoor temperature, the indoor humidity and the supply air temperature are assigned so that $\theta_r = 26°C$, $\varphi_r = 50\%$, and $\theta_{sr} = 10°C$.

The outdoor air temperature θ_0 as disturbance is assumed to be sinusoidal, forcing input with amplitude 5°C and period 10 hours around 32.5°C. Given the same initial conditions, the simulated transient responses are similar to the responses with the constant outdoor temperature. Thus, the outdoor temperature is fixed at 32.5°C.

Tuning of the control parameters is important, and it is desirable to determine approximated values for these parameters from the simplified model. Control parameters can be found by the partial model matching method (Kamimura et al. 1994) for the approximated transfer functions of zone models given by

$$\left.\begin{aligned}\frac{\Theta_3(s)}{F_s(s)} &= \frac{2.5e^{-2.2s}}{1+37.0s},\\ \frac{X_3(s)}{X_d(s)} &= \frac{0.66e^{-2.2s}}{1+2.9s},\\ \frac{\Theta_s(s)}{F_c(s)} &= \frac{1544e^{-0.14s}}{1+2.5s}\end{aligned}\right\}. \tag{21}$$

These time constants are given as a function of the supply airflow rate f_s. For simplicity in this study, these characteristics are based on the fixed airflow rate (i.e., $f_s = 2$ m^3/min) for Equation 21. A detailed derivation of control parameters is given in the appendix. It should be noted that the transfer function to the absolute humidity x_3 can be well defined, but no information regarding φ_3 can be obtained. Thus, final determination of the gain constant in Equation 21 can be made in a trial-and-error by the simulation. The proportional gain k_{c2} must be reduced on the basis of this gain constant. The cases with gain $k_{c2}/50{,}000$ for control provide the stable responses. Table 2 provides the results of having calculated the control parameters by the partial model matching method.

Figure 9 shows the closed-loop responses to stepwise changes in setpoints. This situation is exactly the same as the start-up operation of an HVAC system. The zone temperature θ_3 settles to the setpoint temperature at 26°C. On the other hand, the zone temperatures θ_4 and θ_5 decrease gradually due to the very slow responses of the walls. The slight drops in θ_4 and θ_5 after about $t = 100$ minutes cannot be compensated in this VAV system. It is interesting to note that except for zones 1 and 2 responses give a slow approach to the steady-state values, without overshoot. The tuning technique is designed to give a response with no overshoot. A considerable overshoot and some oscillation before steady-state value is reached have been judged to be undesirable for HVAC systems.

TABLE 2
Tuning Parameters for PI and I-P Controllers

	PI Action	I-P Action
k_{c1} T_{i1}	2.5 37 (min)	2.8 11 (min)
k_{c2} T_{i2}	0.0015 2.9 (min)	0.0017 1.1 (min)
k_{c3} T_{i3}	0.0044 2.5 (min)	0.005 0.72 (min)

The relative humidity φ_3 settles to the setpoint value at 50%. It can be seen that there is some overshoot in the response. This is due to the selection of k_{c2}. Larger than necessary gain causes oscillations; smaller than necessary gain makes the response slower.

It is important to recognize that the absolute control inputs are a little high when comparing the I-P control to the PI control. The I-P control algorithm is known to be a viable strategy to prevent excessively large control input, but both the proportional and the integral gains should be reduced until a satisfactory response is achieved. When looking to the responses of Figure 9, the overall response speed becomes slower, but there is little difference in the overall response (θ_3 and φ_3 for example) between the PI control and the I-P control. Simulated performance characteristics of the VAV system with suitablely tuned PI parameters indicate satisfactory performance, as shown in Figure 9.

Controllable Region on Psychrometric Chart

The psychrometric chart can be used to illustrate the concept of "attainability" (or "controllability" in the control engineering field). To examine the controllability of an HVAC system, we ask the question, "Can the desired state of the air-conditioned room be controlled by particular control inputs?" This can be easily answered by our simulation program.

Many simulation results are made with various setpoint values and constant outdoor conditions. If the final values of θ_3 and φ_3 on the psychrometric chart remain within prescribed ranges (±0.2°C and ±0.5%) around both setpoint values, as θ_r and φ_r, this system can be judged to be controllable. Figure 10 shows four crucial regions with respect to the controllability, marked as I, II, III, and IV. In region I, the system is controllable for both controlled variables θ_3 or φ_3. In region IV, both θ_3 and φ_3 cannot be controlled, whereas in regions II and III, only θ_3 or φ_3 can be controlled directly.

The controllable region I can be formed by projecting straight lines on the psychrometric chart. The highest temperature of the controllable region can be determined by the outdoor temperature because the setpoint value cannot be set beyond the outdoor temperature for a cooling mode. These lines—designated 1, 2, and 3—can be determined by the capacity limits of VAV control elements.

First, the line 1 indicates the lowest possible temperature due to the maximum airflow rate into the space. The relationship between the steady-state values of the input f_s and the output θ_3 can be easily obtained by manual computation. Although the variation in the wall temperature affects the indoor temperature, it is unnecessary to accurately predict it.

Second, the line 2 can be estimated by the relationship between the input p (the evaporation rate of a resident) and the output x_3 when the humidifier is not in operation ($h = 0$). It should be noted that the output x_3 is calculated as a function of the input f_s, and f_s is also a function of the output θ_3. The nonlinear relation between x_3 and θ_3 may be approximated by a linear (i.e., straight line 2) relation within the error limit of 1%.

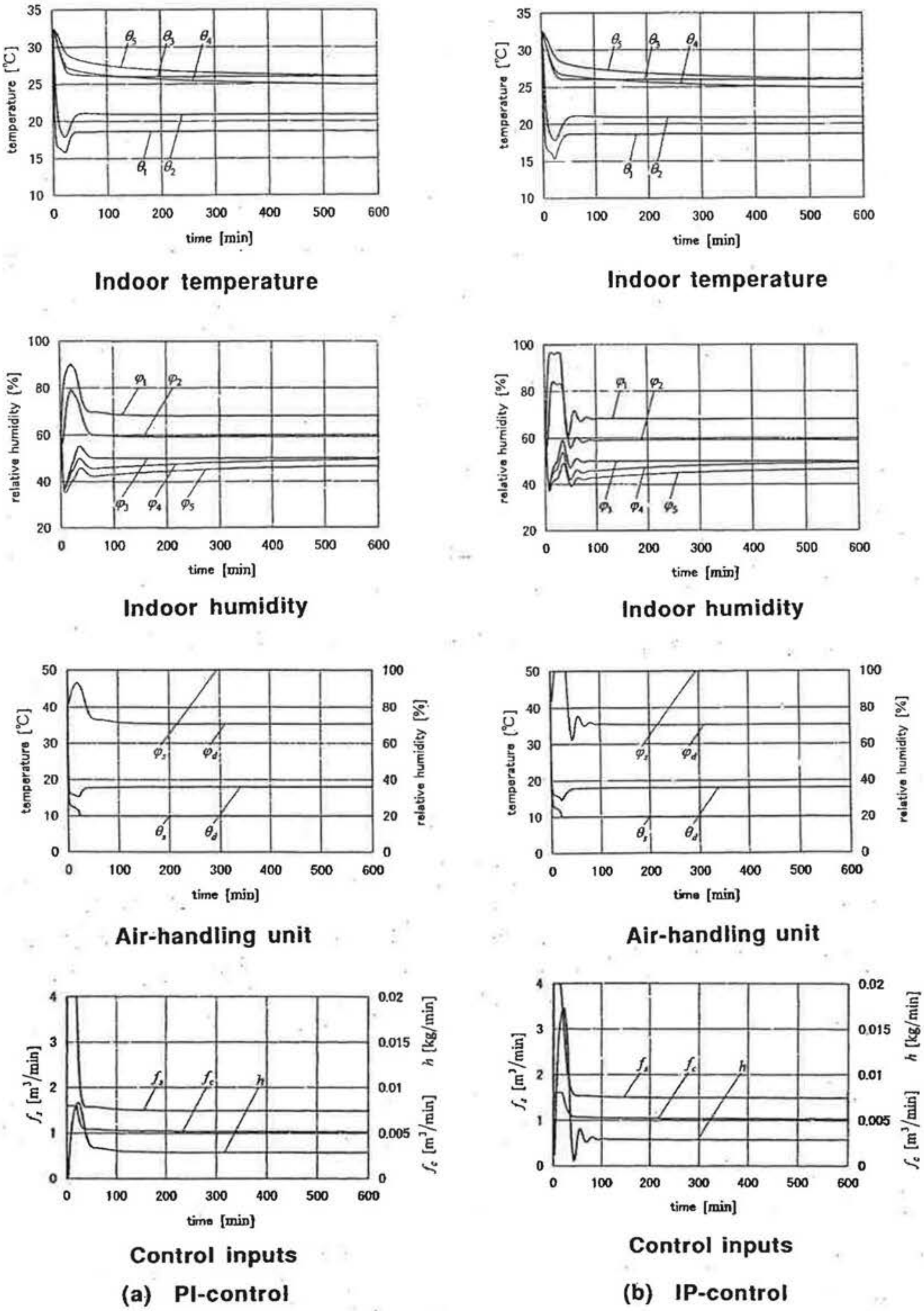

Figure 9 Transient responses of a closed-loop system.

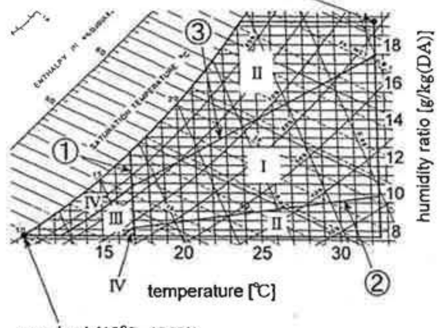

Figure 10 *Controllable region.*

Finally, the line 3 can be estimated similarly. The relation between the supply air temperature in the humidifier θ_d and the supply airflow rate f_s must be estimated when the humidifier is operated at the maximum capacity ($\varphi_d = 100\%$). Note that the humidifier does not always generate maximum power ($h = 0.087$ (kg/min)). By using θ_d, the absolute humidity x_d for saturated vapor can easily be found. The rate of moist air in the humidifier h can be calculated by using x_d and x_s. Consequently, the relation between x_3 and θ_3 may be approximated by a linear function within the error limit of 4%.

All the above simulations were made with the constant outdoor temperature θ_o and the constant supply air temperature θ_s, though in reality the outdoor temperature and thermal loads change constantly. It is interesting to study the effect of varying outdoor temperature and supply air temperature on the controllable region. Figure 11 shows the controllable regions with a changing outdoor temperature with $\theta_o = 32.5\pm2°C$ and a changing supply air temperature with $\theta_s = 10\pm2°C$. With a controlled system, the variation in outdoor temperature has little effect on the controllable region, though the outdoor temperature more or less makes the upper limit of it. It is impractical and unnecessary to accurately compensate for the variation in outdoor temperature. This is exactly the purpose of controls. On the other hand, a supply air temperature lower than 10°C may cause the controllable region to expand, and a temperature higher than 10°C will cause it to increase due to a little amount of temperature rise in the humidifier. The variable supply air temperature can alter the controllable region of the air-conditioning system. Therefore, it is necessary to approximately determine the optimum supply air temperature by the dynamic characteristics of the system.

CONCLUSIONS

By making use of the physical principles of mass and energy balance, a multizone room model has been developed and tested as a VAV control system.

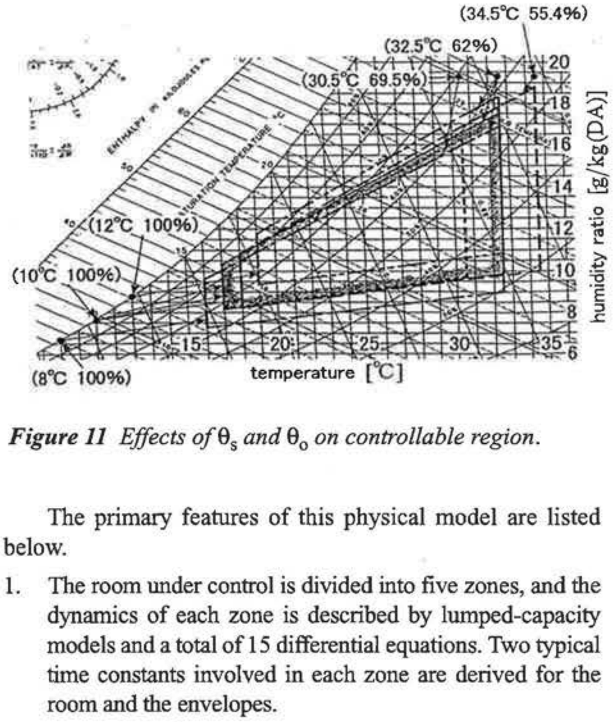

Figure 11 *Effects of* θ_s *and* θ_o *on controllable region.*

The primary features of this physical model are listed below.

1. The room under control is divided into five zones, and the dynamics of each zone is described by lumped-capacity models and a total of 15 differential equations. Two typical time constants involved in each zone are derived for the room and the envelopes.
2. The model parameters derived from this procedure correspond physically to the overall heat transfer coefficients and the thermal capacitances of the room and the envelopes.
3. The systematic method is proposed to replace the higher order system with a well-known first-order lag plus dead time system. The control parameters using PI and I-P control can easily be found for this type of model.
4. To evaluate characteristics of the model, several simulation runs were made. The indoor temperature and the relative humidity for zone 3 can reach the setpoint values in less than about an hour. The transient responses using PI control and I-P control are almost identical. Therefore, it may be

concluded that there is no difference between these two controls in this HVAC system.

5. The resulting system model is especially useful for establishment of the controllable regions on the psychrometric chart.

Although the air-conditioned room is an important element in an HVAC control system, the room often has been assumed with a simple model, such as a first-order lag system, in many application programs. It is, therefore, of significant interest to look closely into room dynamics. The proposed room model in this study provides a theoretical foundation for more elaborate simulations of HVAC control systems. A more detailed model will not only strengthen understanding of the air-conditioned room but enable control engineers to evaluate the overall VAV system.

NOMENCLATURE

C_i = overall thermal capacitance of zone i (kcal/°C)

C_{wi} = overall thermal capacitance of envelope i (including walls, roofs, and floors) (kcal/°C)

C_a = overall thermal capacitance of air-handling unit (kcal/°C)

C_d = overall thermal capacitance of humidifier (kcal/°C)

α_i = overall transmittance-area factor inside zone i (kcal/min °C)

β_i = overall transmittance-area factor outside zone i (kcal/min °C)

α_a = overall transmittance-area factor outside air-handling unit (kcal/min °C)

α_d = overall transmittance-area factor outside humidifier (kcal/min °C)

θ_i = indoor air temperature of zone i (°C)

θ_{wi} = envelope (including walls, roofs, and floors) temperature of zone i (°C)

θ_s = supply air temperature (in air-handling unit) (°C)

θ_d = supply air temperature (in humidifier) (°C)

θ_{si} = mixed air temperature at the inlet of air-handling unit (°C)

θ_o = outdoor air temperature (°C)

θ_{ci} = supply water temperature to cooling coil (4 °C)

θ_{co} = return water temperature to storage tank (9°C)

c_a = specific heat of air (0.24 kcal/kg °C)

c_w = specific heat of cooling water (1.0 kcal/kg °C)

ρ_a = density of air (1.3 kg/m^3)

ρ_w = density of cooling water (998.2 kg/m^3)

$c_a\rho_a$ = heat capacitance of air (0.312 kcal/m^3 C)

f_s = supply airflow rate (4 m^3/min)

f_c = water flow rate through cooling coil (8×10^{-3} (m^3/min)

f_o = outdoor airflow rate (m^3/min)

f_r = return airflow rate (m^3/min)

h = rate of moist air produced in humidifier (0.087 kg/min)

w = product of supply airflow rate and specific heat of air (1.248 kcal/min °C)

w_o = product of outdoor airflow rate and specific heat of air (kcal/min °C)

w_r = product of return airflow rate and specific heat of air (kcal/min °C)

$q(t)$ = non-temperature-dependent heat gain (1.5 kcal/min)

$p(t)$ = evaporation rate of a resident (0.00133 kg/min)

V_i = volume of zone i (m^3)

V_a = volume of air-handling unit (m^3)

V_d = volume of humidifier (m^3)

x_i = indoor absolute humidity of zone i (kg/kg dry air)

x_s = supply air absolute humidity (in air-handling unit) (kg/kg dry air)

x_d = supply air absolute humidity (in humidifier) (kg/kg dry air)

x_{si} = return air absolute humidity at the inlet of air-handling unit (kg/kg dry air)

x_o = outdoor absolute humidity (kg/kg dry air)

φ_i = indoor relative humidity of zone i (%)

REFERENCES

ASHRAE. 1989. *1989 ASHRAE Handbook—Fundamentals.* Atlanta: American Society of Heating, Refrigerating and Air-Conditioning Engineers, Inc.

Åström, K., and T. Hägglund. 1995. *PID controllers: Theory, design and tuning*. Instrument Society of America, pp. 11-27.

Borresen, B.A. 1981. Thermal room models for control analysis. *ASHRAE Transactions* 87 (2): 251-261.

Crawford, R.R., and J.E. Woods. 1985. A method for deriving a dynamic system model from actual building performance data. *ASHRAE Transactions* 91 (1): 1859-1874.

Kamimura, K., et al. 1994. CAT (computer aided tuning) software for PID controllers. *ASHRAE Transactions* 100 (1): 180-190.

Kasahara, M., et al. 1997. A tuning method of two degrees of freedom PID controller. *ASHRAE Transactions* 103 (1): 278-289.

Kimbara, A., et al. 1995. A modeling of an environmental chamber. *ASHRAE Transactions* 101 (1): 262-273.

Kitamori, T. 1980. Design theory, instrumentation and control for PID control systems. *Journal of the Society of Instrument and Control Engineers* 19 (4): 382-391.

Nelson, L.W. 1965. The analog computer as a product design tool. *ASHRAE Journal* 7 (11).

Shavit, G. 1995. Short-time-step analysis and simulation of homes and buildings during the last 100 years. *ASHRAE Transactions* 101 (1): 856-867.

Takahashi, Y., et al. 1972. *Control and dynamic systems.* Addison-Wesley Publishing Company, Inc., pp. 57-64.

Truxal, J.G. 1955. *Automatic feedback control system synthesis.* New York: McGraw-Hill.

Wexler, A., and R.W. Hyland. 1983. *ASHRAE Transactions* 89 (2A): 500.

Zaheer-Uddin, M., and G.R. Zheng. 1994. A VAV system model for simulation of energy management control functions: Off normal operation and duty cycling. *Energy Convers. Mgmt.* 35 (11): 917-931.

Zhang, Z., and R.M. Nelson. 1992. Parametric analysis of a building space conditioned by a VAV system. *ASHRAE Transactions* 98 (1): 43-48.

APPENDIX

PARTIAL MODEL MATCHING METHOD OF DETERMINING PID PARAMETERS

This is a systematic method with which to determine control parameters without estimating roots in such a way that the transfer function of a control system can be as equal to the transfer function of a reference model as possible from the setpoint to the controlled variable (Kitamori 1980).

As a reference model, this work adopts an equation (called a *denominator sequence representation*), as shown below, in accordance with the coefficient sequence of the transfer function.

$$G_m(s) = \frac{1}{\alpha_0 + \alpha_1 \sigma s + \alpha_2 \sigma^2 s^2 + \alpha_3 \sigma^3 s^3 + \dots} \tag{A-1}$$

In this equation, σ is introduced as a scaling factor for time. It is equivalent to the rise time of about 60% of the step response of $G_m(s)$. The response form of the coefficient vector $\{\alpha_i\}$ is given as follows:

$$\{\alpha_i\} = \{1, 1, 0.5, 0.15, 0.03, 0.003, \dots\} \text{ for 10 \% overshoot,} \tag{A-2}$$

and

$$\{\alpha_i\} = \{1, 1, 0.375, 0.0625, 0.0039, \dots\} \text{ for no overshoot)} \tag{A-3}$$

A critically damped response has been selected because it should be adequate for most HVAC applications. Thus, Equation A3 is adopted in this study.

To tune a PID controller, a sequence of parameters suitable to the transfer function of a controlled system is found as a reference model. Each element in a control system needs to be expressed as a quotient of polynominals in s.

If deadtime (L_p) is allowed, the plant transfer function is approximated in the following equation according to the first- or second-order Padé approximations (Truxal 1955):

$$e^{-L_p s} = \frac{1 - \frac{1}{2}L_p s}{1 + \frac{1}{2}L_p s} \quad \text{or} \quad e^{-L_p s} = \frac{1 - \frac{1}{2}L_p s + \frac{1}{12}L_p^2 s^2}{1 + \frac{1}{2}L_p s + \frac{1}{12}L_p^2 s^2} \tag{A-4}$$

Thus, the plant transfer function,

$$G_p(s) = \frac{b_{p0} + b_{p1}s + b_{p2}s^2 + \dots}{a_{p0} + a_{p1}s + a_{p2}s^2 + \dots} \tag{A-5}$$

is represented as a denominator sequence,

$$G_p(s) = \frac{1}{a_0' + a_1' s + a_2' s^2 + \dots}. \tag{A-6}$$

Here, a_0', a_1', a_2', and a_3' are obtained by calculation as in Equation A6.

$$\left.\begin{aligned} a_0' &= a_{p0}/b_{p0},\ a_1' = \{a_{p1} - b_{p1}a_0'\}/b_{p0} \\ a_2' &= \{a_{p2} - (b_{p1}a_0' + b_{p2}a_0')\}/b_{p0} \\ a_3' &= \{a_{p3} - (b_{p1}a_2' + b_{p2}a_0' + b_{p3}a_1')\}/b_{p0} \end{aligned}\right\} \tag{A-7}$$

PID Control Systems. This control structure is represented in the block diagram shown in Figure A1. The controller is given below.

$$G_c(s) = k_c\left[1 + \frac{1}{T_i s} + T_d s\right] = \frac{c_0 + c_1 s + c_2 s^2}{s}. \tag{A-8}$$

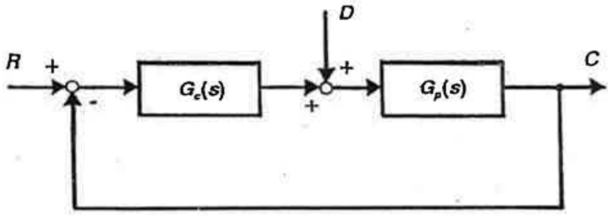

Figure A-1 *PID control system.*

In this equation, $c_0 = k_c/T_i$, $c_1 = k_c$, and $c_2 = k_cT_d$ are represented. The transfer function of a closed-loop system is given in Equation A9.

$$\begin{aligned} W(s) &= \frac{G_c(s)G_p(s)}{1 + G_c(s)G_p(s)} \\ &= \frac{c_0 + c_1 s + c_2 s^2 + c_3 s^3}{c_0 + (c_1 + a_0')s + (c_2 + a_1')s^2 + (c_3 + a_2')s^2 + \dots} \end{aligned} \quad \text{(A-9)}$$

When Equation A9 is equal to Equation A1, which can be solved with respect to c_0, c_1, c_2, and c_3, Equation A10 is obtained.

$$\left.\begin{aligned} c_0 &= \frac{a_0'}{\sigma}, \quad c_1 = \frac{a_0'}{\sigma}\left[\frac{a_1'}{a_0'} - \sigma\alpha_2\right] \\ c_2 &= \frac{a_0'}{\sigma}\left\{\frac{a_2'}{a_0'} - \sigma\alpha_2\frac{a_1'}{a_0'} + \sigma^2(\alpha_2^2 - \alpha_3)\right\} \\ c_3 &= \frac{a_0'}{\sigma}\left\{\frac{a_3'}{a_0'} - \sigma\alpha_2\frac{a_2'}{a_0'} + \sigma^2(\alpha_2^2 - \alpha_3)\frac{a_1'}{a_0'} + \sigma^3(2\alpha_2\alpha_3 - \alpha_2^3 - \alpha_4)\right\} \end{aligned}\right\} \quad \text{(A-10)}$$

The portions after c_1, c_2, and c_3 are eliminated, depending on the I, PI, and PID actions. Therefore, the coefficient of the corresponding term must be zero in Equation A10. For example, if a PI action can be adopted, it can be seen from Equation A10 that the value c_2 (of D action) must be 0. For this reason, the following equations are obtained as equations satisfying σ:

I action:

$$a_1'/a_0' - \sigma\alpha_2 = 0,$$

PI action:

$$a_2'/a_0' - \sigma\alpha_2 a_1'/a_0' + (\alpha_2^2 - \alpha_3), \quad \text{(A-11)}$$

and PID action:

$$\begin{aligned} &a_3'/a_0' - \sigma\alpha_2 a_2'/a_0' + \sigma^2(\alpha_2^2 - \alpha_3)a_1'/a_0' \\ &+ \sigma^3(2\alpha_2\alpha_3 - \alpha_2^3 - \alpha_4) = 0. \end{aligned}$$

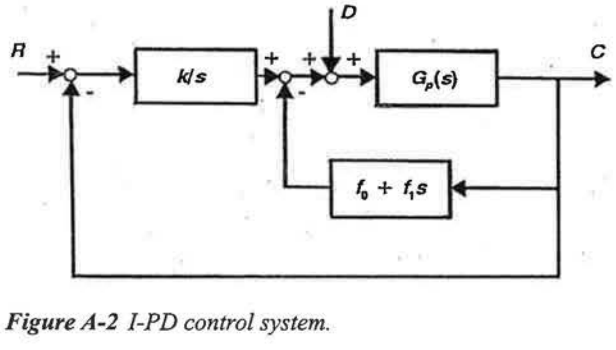

Figure A-2 I-PD control system.

I-PD Control System. This control structure is shown in the block diagram in Figure A2. If the main controller and the feedback compensator are assumed to be

$$G_c(s) = \frac{k}{s}$$

and

$$F(s) = f_0 + f_1 s, \quad \text{(A-12)}$$

the transfer function of the closed-loop system is given in the following equation:

$$\begin{aligned} W(s) &= \frac{1}{1 + \dfrac{1 + F(s)G_p(s)}{G_c(s)G_p(s)}} \\ &= \frac{1}{1 + \dfrac{a_0' + f_0}{k}s + \dfrac{a_1' + f_1}{k}s^2 + \dfrac{a_2'}{k}s^3 + \dfrac{a_3'}{k}s^4 + \dots} \end{aligned} \quad \text{(A-13)}$$

When Equation A13 is equal to Equation A1, the following equations are used:

$$\begin{aligned} &\frac{a_0' + f_0}{k} = \sigma, \qquad \frac{a_1' + f_1}{k} = \alpha_2\sigma^2, \\ &\frac{a_2'}{k} = \alpha_3\sigma^3, \qquad \text{and} \qquad \frac{a_3'}{k} = \alpha_4\sigma^4. \end{aligned} \quad \text{(A-14)}$$

Therefore, the following parameters are obtained:

$$\begin{aligned} &\sigma = \frac{\alpha_3 a_3'}{\alpha_4 a_2'}, \qquad k = \frac{a_2'}{\alpha_3\sigma^3}, \\ &f_0 = \sigma k - a_0', \qquad \text{and} \qquad f_1 = \alpha_2\sigma^2 k - a_1' \end{aligned} \quad \text{(A-15)}$$

This I-PD system has proved effective for a disturbance input (Kitamori 1980).

Example of Execution. To illustrate the computational trials, the indoor temperature control is considered as an example in the following.

$$G_p(s) = \frac{K_p e^{-L_p s}}{1 + T_p s}$$

where $K_p = 2.5$, $T_p = 37$, and $L_p = 2.2$.

The plant transfer function can be represented as the following denominator sequence,

$$G_p(s) = \frac{1}{a_0' + a_1's + a_2's^2 + \dots},$$

where $a_0' = 1/K_p$, $a_1' = (L_p + T_p)/K_p$, $a_2' = \left(\frac{L_p}{2} + T_p\right)L_p/K_p$, and $a_3' = \left(\frac{L_p}{6} + \frac{T_p}{2}\right)L_p^2/K_p$.

PID Control. From approximations, the parameters in Equation A10 are given as

$$\sigma = 1.37L_p = 3.03$$

$$c0 = a_0'/\sigma = 0.132$$

$$c_1 = c_0\left(\frac{a_1'}{a_2'} - \sigma\alpha_2\right) = 5.027$$

$$c_2 = \left\{\frac{a_2'}{a_0'} - \sigma\alpha_2\frac{a_1'}{a_0'} + \sigma^2(\alpha_2^2 - \alpha_3)\right\} = 5.344$$

Thus, PID parameters can be easily obtained as

$k_c = c_1 = 5.027$, $T_i = c_1/c_0 = 38.08$, and $T_d = c_2/c_1 = 1.063$.

Similarly, for the PI mode, the parameters are

$$\sigma = 5.95,\ c_0 = 0.06728,\ c_1 = 2.498.$$

Thus, PI parameters can be found as

$k_c = 2.489$ and $T_i = 36.99$.

I-PD Control. Substituting plant parameters into Equation A15, we found the parameters for I-PD control to be

$$\sigma = \frac{\alpha_3 a_3'}{\alpha_4 a_2'} = 17.57,\ k = \frac{a_2'}{\alpha_3\sigma^3} = 0.09962,$$

$$f_0 = \sigma k - a_0' = 1.35, \text{ and } f_1 = \alpha_2\sigma^2 k - a_1' = -4.168.$$

It should be noted that a derivative action f_1 for the reference model with no overshoot cannot be found as a positive number. Thus, the I-P control model must be adopted. We found the parameters for I-P control to be

$$\sigma = \frac{\alpha_2 a_2'}{\alpha_3 a_1'} = 12.91,\ k = \frac{a_1'}{\alpha_2\sigma^2} = 0.2512,$$

$$\text{and } f_0 = \sigma k - a_0' = 2.843.$$